SCIENCE CHINA
Earth Sciences

•RESEARCH PAPER•

April 2020 Vol.63 No.4: 575–590
https://doi.org/10.1007/s11430-018-9532-5

Evaluation of the glacial isostatic adjustment (GIA) models for Antarctica based on GPS vertical velocities

Fei LI, Chao MA, Shengkai ZHANG*, Jintao LEI, Weifeng HAO, Qingchuan ZHANG & Wenhao LI

Chinese Antarctic Center of Surveying and Mapping, Wuhan University, Wuhan 430079, China

Received March 27, 2019; revised September 11, 2019; accepted October 22, 2019; published online January 2, 2020

Abstract Due to the scarcity of data, modeling the glacial isostatic adjustment (GIA) for Antarctica is more difficult than it is for the ancient ice sheet area in North America and Northern Europe. Large uncertainties are observed in existing GIA models for Antarctica. Modern space-based geodetic measurements provide checks and constraints for GIA models. The present-day uplift velocities of global positioning system (GPS) stations at 73 stations in Antarctica and adjacent regions from 1996 to 2014 have been estimated using GAMIT/GLOBK version 10.5 with a colored noise model. To easily analyze the effect of difference sources on the vertical velocities, and for easy comparison with both GIA model predictions and GPS results from Argus et al. (2014) and Thomas et al. (2011), seven sub-regions are divided. They are the northern Antarctic Peninsula, the Filchner-Ronne Ice Shelf, the Amundsen Sea coast, the Ross Ice Shelf, Mount Erebus, inland Southwest Antarctica and the East Antarctic coast, respectively. The results show that the fast uplift in the north Antarctic Peninsula and Pine Island Bay regions may be caused by the elastic response to snow and ice mass loss. The fast subsidence near Mount Erebus may be related to the activity of a magma body. The uplift or subsidence near the East Antarctic coast is very slow while the uplift for the rest regions is mainly caused by GIA. By analyzing the correlation and the associated weighted root mean square (WRMS) between the GIA predictions and the GPS velocities, we found that the ICE-6G_C (VM5a) model and the Geruo13 model show the most consistency with our GPS results, while the W12a and IJ05_R2 series models show poor consistency with our GPS results. Although improved greatly in recent years, the GIA modeling in Antarctica still lags behind the modeling of the North American. Some GPS stations, for example the Bennett Nunatak station (BENN), have observed large discrepancies between GIA predictions and GPS velocities. Because of the large uncertainties in calculating elastic responses due to the significant variations of ice and snow loads, the GPS velocities still cannot be used as a precise constraint on GIA models.

Keywords Antarctica, GPS, Glacial isostatic adjustment, Vertical velocity, Uncertainty

Citation: Li F, Ma C, Zhang S, Lei J, Hao W, Zhang Q, Li W. 2020. Evaluation of the glacial isostatic adjustment (GIA) models for Antarctica based on GPS vertical velocities. Science China Earth Sciences, 63: 575–590, https://doi.org/10.1007/s11430-018-9532-5

1. Introduction

Long-term motion in Antarctica mainly consists the three-dimensional deformation due to past and present changes in ice-ocean mass, which is called glacial isostatic adjustment (GIA), and the horizontal plate tectonic (King and Santamaría-Gómez, 2016). Because most GIA models do not consider ice mass changes of the last 2000 years (Nield et al., 2015), the GIA in this study only means the responses of viscoelastic earth to the load changes of surface ice and sea water in the last glacial maximum (21–6 ka B.P.), which is also known as postglacial rebound. The Last Glacial Maximum (LGM) occurred approximately 21 ka B.P., and the ice sheets in Antarctica, North America and so on began to melt at that time and stopped melting at ~6 ka B.P. The net sea-level rise during the LGM and the interglacial period was at

* Corresponding author (email: zskai@whu.edu.cn)

approximately 120–130 m (Peltier, 2004). The mass redistribution of ice and ocean mass cause the significant redistribution of the Earth's surface loads, impacting the gravity field and the rotation of the Earth, causing a surface deformation due to the viscoelastic response of the Earth (Mitrovica et al., 2009). Data on glacier geology and ancient sea levels can provide constraints on the history of such deformation and mass redistribution. GIA models can provide important corrections for studies such as the plate tectonics, crustal vertical movement, geoid change, sea-level change, Gravity Recovery and Climate Experiment (GRACE) gravity field solutions, satellite altimetry (Wang et al., 2008; Ivins et al., 2013; Prandi et al., 2009). Accompanied with GPS and VLBI, GIA can help establish a robust international terrestrial reference frame (Altamimi and Collilieux, 2009), and provides the boundary conditions at the edge of marine-grounded regions (Whitehouse et al., 2012a).

A comparison of several current GIA models identified considerable differences between the models, such as in the Antarctic ice sheet region, where the differences of uplift velocities in GIA models can exceed several mm yr^{-1}. The reason for the large uncertainty in GIA models is due to the lack of constrained data at present. The uncertainties of GIA models are mainly based on two aspects: inaccurate ice thickness histories and greatly simplified Earth models. The three relevant parameters of GIA models are the thickness of the ice sheet, the thickness of the elastic lithosphere and the viscosity of the mantle. Errors in any one of these parameters may affect the estimations of the other two parameters (Argus et al., 2014). Seismic data have shown that there are drastic viscosity variations in the Antarctic mantle, however, most GIA models assume that the viscosity of Antarctic mantle is radially stratified. Ignoring the transverse non-uniformity of viscoelasticity would introduce potential errors which may affect the predictions of the GIA models (Wang and Wu, 2006; Wu and Wang, 2006; Wang et al., 2008).

The Earth's mantle viscosity dominates the response time of Earth adjustments. The high viscosity of the Antarctic mantle make it possible for the adjustments to be observed today, in which the the obvious surface deformation and gravity changes can be observed by geodesy and geophysical instruments. Therefore, current geodetic and geophysical measurements of GIA can provide insights into past ice sheet structures and sea level change, as well as the Earth's structure and rheology (Milne et al., 2001; King et al., 2010). High-precision crustal motion velocity obtained using continuous GPS measurements offers the potential for external verification and new constraints on GIA models. Most of the International GNSS Service (IGS) continuous stations in Antarctica are built on the scientific research stations of various countries and basically distributed in the coastal areas of Antarctica. Since the beginning of the 1990s, the international Scientific Committee of Antarctic Research (SCAR) has established the West Antarctic GPS Network (WAGN), Trans Antarctic Mountains Deformation (TAMDEF), Victoria Land Network for Deformation Control (VLNDEF) and other GPS geodetic networks. In the 2007–2008 International Polar Year, the Polar Earth Observing Network (POLENET) program was implemented in Antarctica by multinational cooperation. This program's main task is to deploy continuous observation instruments, such as GPS and seismometers, for earth science research in the polar regions (E and Zhang, 2006). In recent years, with the implementation of the POLENET program and the continuous expansion of the Antarctic IGS stations, the number of continuous GPS stations in the Antarctic has been greatly improved in both quantity and distribution, which makes using the GPS data with longer sequences and higher observation accuracies to test and constrain the GIA models become possible.

2. GPS data processing

2.1 GPS data sources

To accurately estimate the vertical velocities and precision of the GPS stations, the time span of GPS time series should be longer than 2.5 years (Blewitt and Lavallée, 2003). In total, 73 GPS stations were selected in this study, in which 65 stations are located in Antarctica (south of 60°S, including 12 IGS stations, 39 stations POLENET, 6 Antarctica Erebus (AE) GPS network stations, a Chinese station (Zhongshan, ZHON), and 7 stations from other networks) (Figure 1). Eight stations in adjacent areas (north of 60°S) were used as the reference stations for baseline processing and network adjustment. The time spans are from 1996 to 2014, and the longest time span is approximately 19 years.

2.2 Baseline processing

The raw GPS data were processed using GAMIT/GLOBK10.5. Since the number of stations to be processed is as many as 73, the solution efficiency of the whole network is very low. Jiang et al. (2011) pointed out that although subnetting all processed stations will theoretically affect the rigor of the mathematical model, but the impact is small in actual calculations and the accuracy is comparable to that of a whole-net solution. When processing the global GPS network, the Scripps Institute of Oceanography (SIO) also divided the global network into multiple subnets and performed baseline processing for each subnet and then combined them all to adjustment. In this paper, we divided the whole network into 3 subnets (there are at least 6 public sites between subnets) and then uniformly adjusted them. The solution type is a relaxation solution (RELAX), and the satellite orbit is calculated at the same time. The coordinates

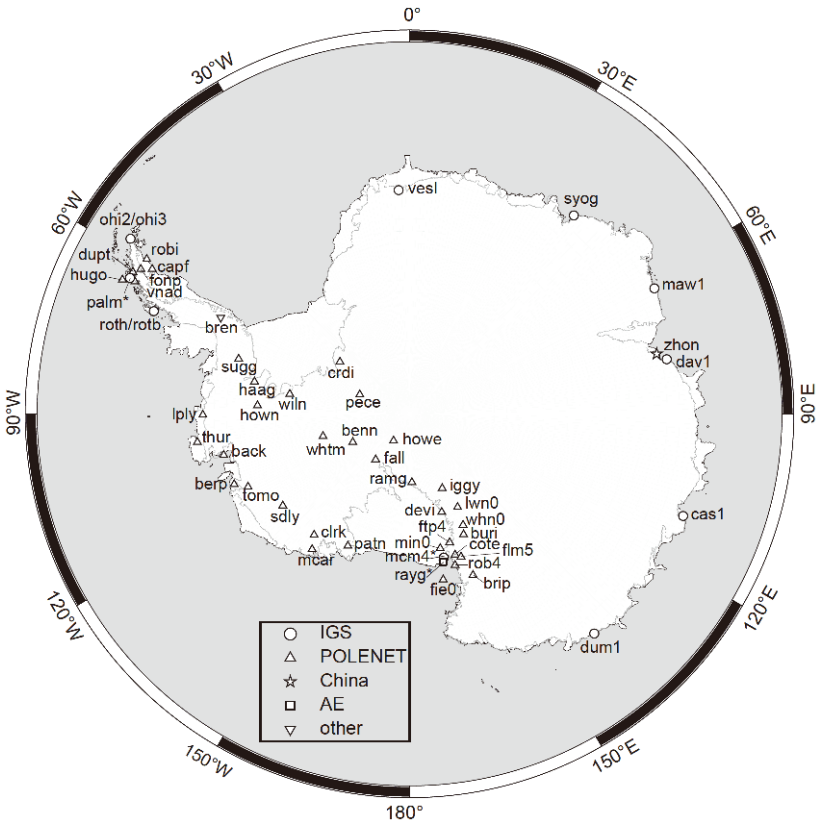

Figure 1 The distribution of 65 continuous GPS stations in the Antarctic region (south of 60°S), where the circle represents the IGS station, the triangle represents the POLENET station, the pentagram represents the Zhongshan station (ZHON), and the rectangle represents the Antarctic Eribos volcano GPS. Some stations that are close to each other are named as one station with "*": palm* represents palm/palv/pal2; mcm4* represents mcm4/crar/mcmc/mcmd, rayg* represents rayg/naus/lehg/e1g2/cong/hooz/macg.

of the station are calculated. The observations use the combination of no ionosphere and the automatic repair of the cycle slip mode (LC_AUTCLN). The station prior coordinate constraints are as follows: the IGS station constraints are 0.05, 0.05, and 0.10 m and other station constraints are 100, 100, and 100 m. In addition, the elevation cutoff is 15°; the epoch interval is 30 s; the tropospheric delay correction is accomplished using the Saastamoinen model; tidal correction is using the 2004 finite element solution (FES2004) model; the Berne model is used for the radiation perturbation correction; the reference frame is the 2008 International Terrestrial Reference System (ITRF2008); and the other parameters are the default settings in GAMIT/GLOBK10.5 (Ma et al., 2016).

2.3 Network adjustment

After baseline processing completed, GLOBK was used to perform the network adjustment and calculate the final coordinates time series in the ITRF2008 framework. Because the GPS network in this paper was regional, to maintain the stability of the framework, we merged our results with the baseline solutions of the global IGS networks IGS1–IGS9 (downloaded from the Scripps Orbit and Permanent Array Center (SOPAC) at ftp://garner.ucsd.edu/archive/garner/solutions/global/) to perform a combined adjustment. In total, 91 core stations with IGS08 antenna calibrations (IGb08) were selected as frame stabilization stations, and the coordinates of the stabilization stations north (N), east (E) and up (U) were constrained to 0.01, 0.01 and 0.05 m, respectively; the horizontal coordinates and its associated error constraints of the poles were 0.25, 0.25, 0.1, 0.1 m, respectively. The UT1 and its associated error constraints were 0.25 and 0.1 s, respectively. After adjustment, the repeatability of the horizontal component (Weighted Root Mean Squared, WRMS) of the GPS time series for each station was better than 5 mm, and the repeatability of the vertical component better than 10 mm (Li et al., 2016).

2.4 Elimination of outliers

A few outliers are observed in the time series obtained by the GLOBK network adjustment, and they may be caused by changes in the external environment or the changes of instruments. These outliers will cause deviations in the time series analysis; therefore, it is necessary to eliminate them. In

this paper, we use the interquartile range (IQR) (Nikolaidis, 2002) to eliminate outliers in the coordinate time series. The criteria for eliminating outliers are as follows:

$$\left|\hat{x}_i - \text{median}(x_{i-w/2,\, i+w/2})\right| > 3 \cdot \text{IDR}(x_{i-w/2,\, i+w/2}), \quad (1)$$

where $\hat{x}_i$ represents the coordinate of the station at the i-th epoch, w is the width of the time window, $\text{median}(x_{i-w/2,\, i+w/2})$ represents the median in the window centered on the i-th epoch and $\text{IDR}(x_{i-w/2,\, i+w/2})$ represents the difference in the quantiles in the window. First, the time series in the window are arranged from smallest to largest, and then the IQR is obtained by taking the difference between the 75th and 25th percentiles. The width of the time window w is 1 year in this paper.

2.5 Corrections of offsets

The time series of some GPS stations show step mainly due to earthquake or antenna change. In this paper, the epoch and the magnitude of the step corrections are obtained using the coordinates before and after the step from the seismic data files provided by GAMIT/GLOBK10.5. After corrections, there are still steps in the time series of the Whitmore Mountains (WHTM) station. In this paper, the coordinate time series before and after the step is fitted by CATS and the jump in the coordinate fitting before and after the step (i.e., the step value) is calculated. Then, the coordinates after the step are corrected using the jump value. The time series of coordinates before and after the step correction of WHTM is shown in Figure 2. A 30-mm jump in the U-direction coordinate time series of epoch 2011.978 is observed. After step correction, the vertical velocity and error estimation of the station decreased obviously. The velocity decreased from 13.65 to 4.38 mm yr^{-1}, and the error decreased from 3.66 to 1.66 mm yr^{-1}.

2.6 Velocity estimation and combination

Not only white noise but also colored noise occurs in the GPS position time series, and such noise has an important influence on parameter estimation (Jiang and Zhou, 2015). Li et al. (2014) analyzed the coordinate time series of the 12 IGS stations on the Antarctic continent and found that the optimal noise model in the Antarctic region is white noise (WN)+flicker noise (FN)+random walk noise (RWN). Therefore, the velocities and errors of the 73 stations in this paper for the N, E and U components were estimated by using the maximum likelihood estimation method with WN, FN and RWN considered simultaneously. Because some stations are very close to each other (within 5 km), although the velocity of each station is not the same, they can be considered colocated stations and merged into one time series. There are four groups of colocated stations in this paper. As shown in Table 1, the weighted average velocities of the colocated stations were calculated to represent the average velocities by weighting the reciprocal of the errors in the velocities of the stations. To distinguish the merged stations from the premerged stations and facilitate their future use, the merged stations are named McMurdo* (MCM4*), Palmer* (PALM*), O'Higgins* (OHI2*) and Rothera* (ROTH*). After merging, there are a total of 66 stations, 58 of which are on the Antarctic continent and 8 are

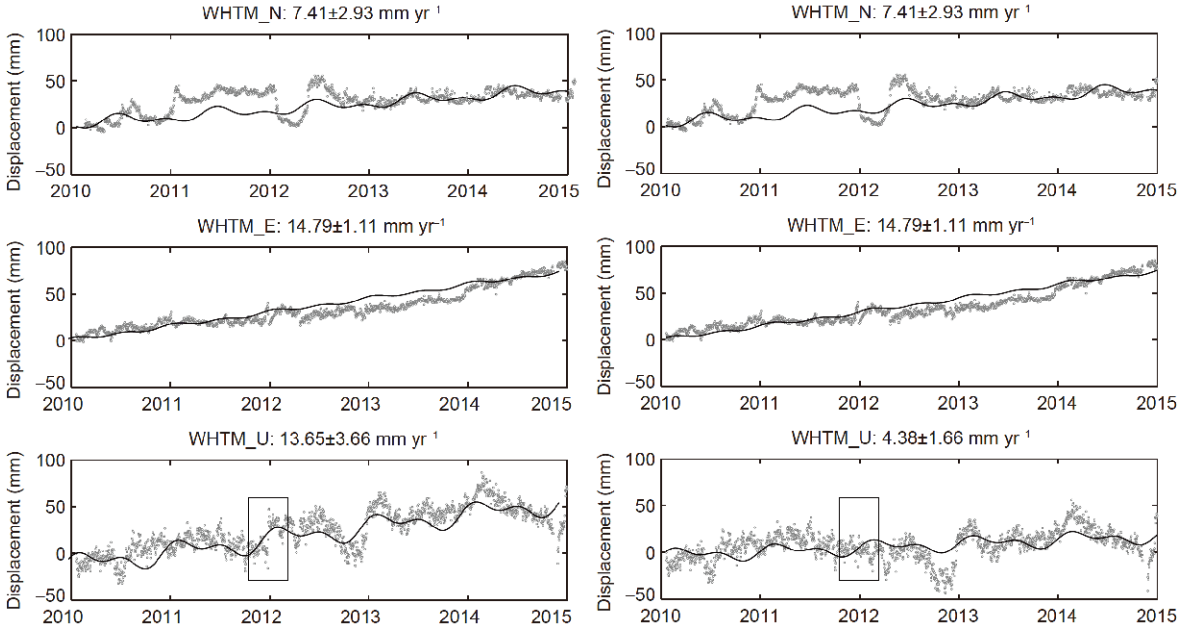

Figure 2 Comparison of time series between before and after the step correction. The gray point is the time series, the black solid line is the fitting result of the linear and periodic term, and the box is the step correction.

Table 1 Combined vertical velocities of co-location stations

Station	Longitude	Latitude	V_u (mm yr^{-1})	ΔV_u (mm yr^{-1})	v' (mm yr^{-1})
CRAR	166.67°E	77.84°S	0.66	0.34	0.69
MCM4	166.67°E	77.84°S	0.62	0.26	
MCMC	166.67°E	77.84°S	0.99	0.56	
MCMD	166.67°E	77.84°S	0.77	0.56	
PAL2	64.05°W	64.78°S	6.31	0.64	6.18
PALM	64.05°W	64.78°S	6.08	0.33	
PALV	64.05°W	64.78°S	6.28	1.11	
OHI2	57.90°W	63.32°S	3.17	1.14	3.15
OHI3	57.90°W	63.32°S	3.09	3.26	
ROTB	68.13°W	67.57°S	3.46	0.97	4.11
ROTH	68.13°W	67.57°S	5.45	2.00	

not on the Antarctic continent. Since the focus of this study is on the Antarctic region, the next section will focus on the analysis of the velocities of the GPS stations in Antarctica.

2.7 Influence of the different reference frames

To accurately compare and analyze the GPS vertical velocities and the predictions of the GIA model, the reference frames must be the same or consistent. The origin of the reference frame of the GIA model is the mass center of the solid earth (CE), while the GPS velocities are estimated in the ITRF2008 reference frame, whose origin is the mass center of the total earth system (CM). Thomas et al. (2011) estimated the differences of the reference frame between ITRF2005 and ICE-5G and found that the differences in the X, Y and Z components are only -0.2 ± 0.1, 0.0 ± 0.1 and -0.1 ± 0.1 mm yr^{-1}, respectively. Argus et al. (2014) also found that the velocities between CM and CE caused by GIA are very small, whereas the velocities caused by modern ice mass loss are more significant. If Greenland had an ice loss of 200 Gt yr^{-1} and the other areas had no ice loss, then the velocity should be approximately 0.22 mm yr^{-1}. The above corrections are much smaller than the uncertainties in the GIA models and GPS vertical velocities; therefore, the impact of these corrections on this study can be ignored.

3. Analysis of vertical movement in different regions

The factors causing the vertical movement in Antarctica are not entirely GIAs but also changes in the ice and snow load and the geological structure. At present, there are two methods of addressing the elastic response caused by changes in the ice and snow load. One method is to eliminate the influence of the change in the ice and snow load by establishing the elastic response model to correct the GPS velocity elastically. The other method is to directly exclude the areas where obvious changes in the ice and snow load exist. Because the current elastic response model is similar to the GIA model, there are still large uncertainties, especially in areas where the ice and snow loads vary significantly, although these areas are usually excluded when geodetic data are used to test or constrain GIA models (Thomas et al., 2011; Ivins et al., 2013; Argus et al., 2014). In other regions where the change is not significant, the effect of the elastic response model correction is negligible (Argus et al., 2014). Therefore, we eliminated or weakened the influence of observations in areas where significant changes in the ice and snow load and the active tectonic movement exist. To compare and analyze the influence of different factors, the Antarctic continent is divided into seven regions according to the influence degree and the geographical location of each factor, including the northern Antarctic Peninsula, Weddell Sea coast, Amundsen Sea coast, Ross Sea coast, Mount Erebus, West Antarctic inland and East Antarctic coast regions. The vertical movement characteristics of each region are discussed and analyzed based on the presence or absence of an apparent loss of ice mass or strong tectonic activity. Figure 3 shows the comparison of the GPS vertical velocities of 58 stations in this study with the GPS results from Thomas et al. (2011) and Argus et al. (2014) as well as the predictions from nine GIA models: ICE-6G_C (VM5a) (Argus et al., 2014; Peltier et al., 2015), ICE-5G (VM2_L90) (Peltier, 2004; Argus and Peltier, 2010), W12a (Whitehouse et al., 2012a, 2012b), Geruo13 (Geruo et al., 2013), IJ05_R2 (Ivins et al., 2013) and Paulson07 (Paulson et al., 2007). The Geruo13 model has three submodels based on different truncation orders and Gaussian filtering radii: (a) truncated to 100 order and no Gaussian filtering; (b) truncated to 60 order and 200 km Gaussian filtering; and (c) truncated to 40 order and 500 km Gaussian filtering. The IJ05_R2 model has two submodels based on different earth model parameters: (a) a lower mantle viscosity of 1.5×10^{21} Pa s and a lithospheric

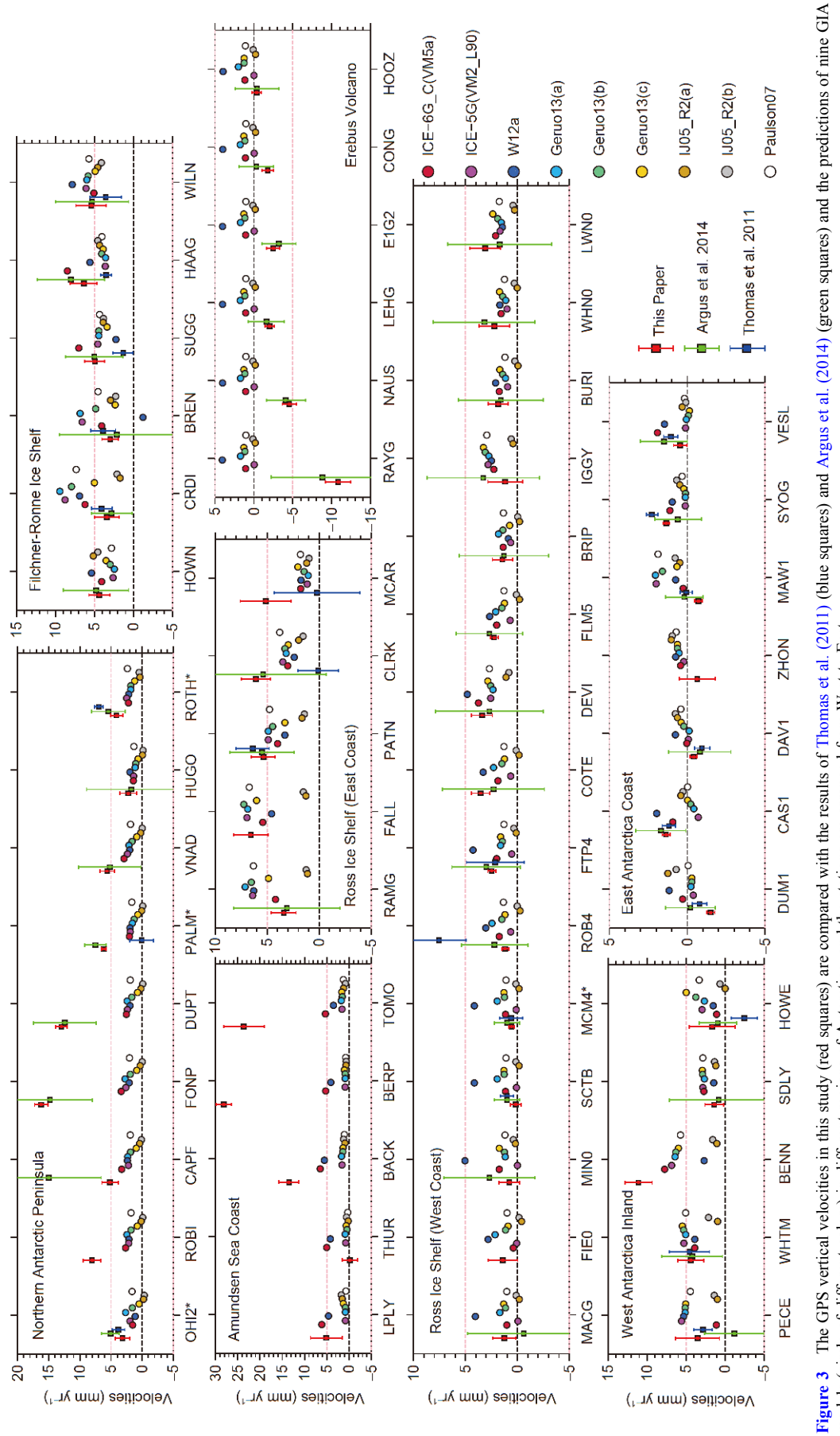

Figure 3 The GPS vertical velocities in this study (red squares) are compared with the results of Thomas et al. (2011) (blue squares) and Argus et al. (2014) (green squares) and the predictions of nine GIA models (circle of different colors) in different regions of Antarctica, and the stations are arranged from West to East.

thickness of 65 km; and (b) lower mantle viscosity of 4×10^{21} Pa s and a lithospheric thickness of 115 km. There are 47 stations that are the same as those in the study by Argus et al. (2014), and there are 24 stations that are the same as those in the study by Thomas et al. (2011). That is, there are at least 11 new stations in this paper. Argus et al. (2014) and Thomas et al. (2011) used GPS data from 1994–2012 and 1995–2010, respectively, while we used GPS data of 1996–2014, i.e., relatively new GPS data.

The length of the error bar in Figure 3 shows that the accuracy of our GPS vertical velocities is much higher than that of other GPS stations and our GPS results are in good agreement with those of the other two studies; however, differences are also between the results of individual stations, such as Cape Framnes (CAPF) and Cape Roberts (ROB4). CAPF is located in the north of the Antarctic Peninsula. Argus et al. (2014) estimated its vertical velocity using two-year data as 15.0±8.4 mm yr^{-1}, while we estimated its velocity using five-year data (2010 to 2014) as 5.18 ±1.29 mm yr^{-1}; the difference between these two estimates is 10 mm yr^{-1}. ROB4 is located in the west of the Ross Ice Shelf. The vertical velocity of ROB4 is estimated as 1.17±0.33 mm yr^{-1} in this paper, which is close to the 2.22±3.20 mm yr^{-1} estimated by Argus et al. (2014) but quite different from the 7.54±2.59 mm yr^{-1} estimated by Thomas et al. (2011). This paper uses 10-year data, and Argus et al. (2014) and Thomas et al. (2011) used 6-year data. However, Thomas et al. (2011) used only 558 days of data. The above differences show that the time span of the data has a very important influence on the estimation of the station velocity. If the time span is too short, there will be great uncertainty in the estimation of station velocity.

3.1 Northern Antarctic Peninsula

The vertical velocities of the GPS stations in the northern Antarctic Peninsula are generally larger than those predicted by GIA models. The vertical velocity at the Foyn Point (FONP) station is the largest, reaching 16.19 mm yr^{-1}, while that of the GIA model at this station is only 3.37 mm yr^{-1}. Such a large gap is unlikely to be caused by the uncertainty in the GIA models; therefore, other reasons must explain the uplift in this area. In 1995, the Prince Gustav Channel and the Larsen A Ice Shelf on the Antarctic Peninsula collapsed, and in 2002, the Larsen B Ice Shelf collapsed. The results show that the glaciers that were surrounded and blocked by the Larsen B Ice Shelf began to lose mass more rapidly due to the collapse of the ice shelf and the major inflow sources of the ice shelf suffered a significant loss of quality. Figure 4 shows the vertical velocity distribution of the GPS stations in the Antarctic Peninsula. FONP is the closest to the collapse area of the Larsen B Ice Shelf, and the maximum uplift velocity is obtained. The velocities of other remote stations

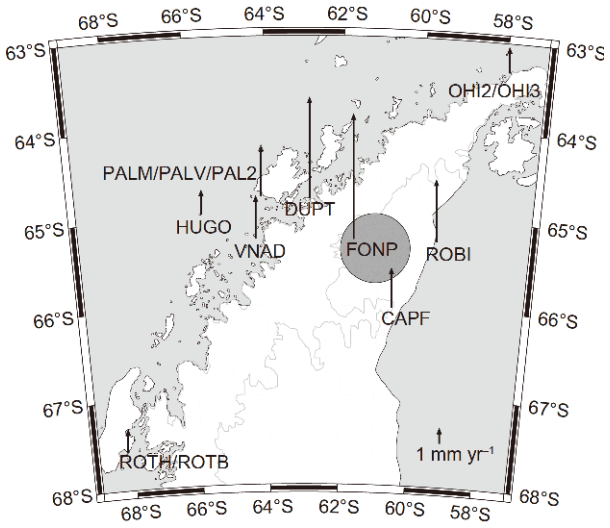

Figure 4 The GPS vertical velocities in Antarctic Peninsula (the arrows' direction represents the rising or descending and their sizes represent the magnitude of velocities). The dotted line represents the land boundary line (not including ice shelf) in Antarctic Peninsula and the circular gray area represents the approximate area of the Larsen B ice shelf collapsed in 2002.

are relatively small, which shows that the collapse of the ice shelf has a great influence on the crustal uplift in this area. Thomas et al. (2011) analyzed the coordinate time series of the OHI2, PALM and ROTH stations in the northern Antarctic Peninsula and found that the coordinate time series had obviously different slopes (velocities) around 2002, especially the uplift velocity at the PALM station, which was only 0.1 mm yr^{-1} before 2002 and reached 8.8 mm yr^{-1} after 2002. The variation in the lift velocity at PALM estimated in this paper is shown in Figure 5. It was 1.80 mm yr^{-1} in 1998–2001 and 6.08 mm yr^{-1} in 2002–2014, which is slightly less than that calculated by Thomas et al. (2011), although the increasing trend is consistent. The vertical velocity at PALM before 2002 (1.8 mm yr^{-1}) is in good agreement with the predicted velocity from each GIA model. This finding shows that the vertical velocity at PALM before 2002 is mainly affected by GIA but is less affected by the change in the current ice and snow load.

3.2 Filchner-Ronne Ice Shelf

The Filchner-Ronne Ice Shelf region consists of one station (Brenekke Nunatak, BREN) in the southern Antarctic Peninsula and five stations along the southern coast. In this region, the results of this paper are very similar to those from Argus et al. (2014), although the results from Thomas et al. (2011) are quite different at Mt. Sugg (SUGG) and Haag Nunataks (HAAG). The reason for these discrepancies may be related to the different time spans of the data used. Thomas et al. (2011) used GPS data from SUGG and HAAG

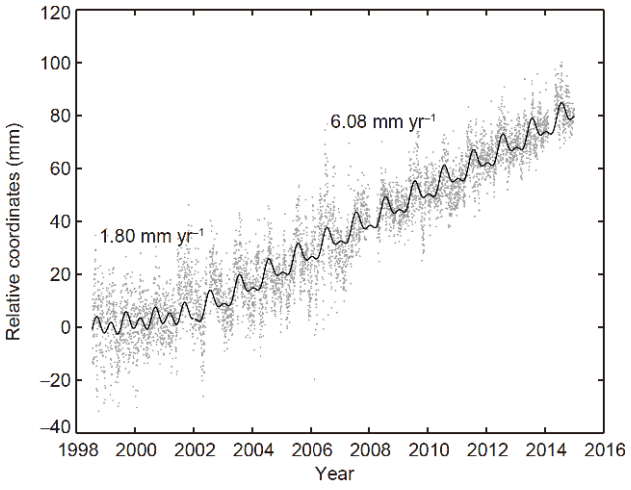

Figure 5 The uplift velocity change of PALM before and after 2002.

from 2003 to 2006, while this paper and Argus et al. (2014) both used GPS data from after 2006. The predicted values of the vertical velocity of GIA in this region basically hover around the vertical velocities of the GPS stations. The GPS results in this paper are in good agreement with the predicted values of most GIA models. Therefore, this paper holds that the main reason for crustal uplift along the Filchner-Ronne Ice Shelf is GIA and not the change in the current ice and snow load, which is similar to the conclusions of Argus et al. (2014). The predictions of some GIA models differ greatly from each other in this region and can reach approximately 8 mm yr^{-1} at BREN. The predictions of the W12a, ICE-5G (VM2_L90) and Geruo13 (a) models for the Cordiner Peak (CRDI) and BREN stations are quite different from those of GPS, which indicates that these GIA models have great uncertainty in this area.

3.3 Amundsen Sea coast

Since all five stations in the Amundsen Sea coastal area were established after 2011, Argus et al. (2014) and Thomas et al. (2011) did not include these stations in their analyses. The data from these stations in this paper have a time span of 3–4 years, which can meet the requirements of crustal motion velocity estimation. The vertical velocity range of the GPS stations along the Amundsen Sea is −0.17 mm yr^{-1} (Thurston Island, THUR) ~28.13 mm yr^{-1} (Bear Peninsula, BERP). The vertical velocities at different GPS stations vary greatly. The predicted values of each GIA model are relatively stable in this area. The predicted values from the ICE-6G_C (VM5a) and W12a models are relatively large at approximately 5 mm yr^{-1}, and the predicted values from other GIA models are also relatively large. The predicted values are relatively small, ranging from 0 to 2 mm yr^{-1}. The predicted values from the Lepley Nunatak (LPLY) and THUR stations are in good agreement with each GIA model, which indicates that their vertical velocity is mainly related to GIA. The lifting velocities of at the Backer Island (BACK), BERP and Toney Mountain (TOMO) stations are much higher than those predicted by all the GIA models, which may be related to the obvious changes in the ice and snow load in the region.

Stations BACK, BERP and TOMO are located in Pine Island Bay. Studies show that the two glaciers in this area, Pine Island Glacier and Thwaites Glacier, are experiencing rapid ice and snow mass loss. Pine Island Glacier is the largest and fastest-moving glacier in Antarctica. Satellite surveys from 2004 showed that surface ice flowed into the Amundsen Sea 25% faster than it did 30 years ago. The bottom of the Thwaites Glacier is one of the largest ice streams in southwest Antarctica, with a very large network of fast-flowing, low-lying waterways. This region is the largest area of ice mass loss in Antarctica. The abnormally large velocities of these three stations reflect the elastic uplift caused by the current ice mass loss in the region.

3.4 Mount Erebus

Mount Erebus is an active volcano located on Ross Island, southwest of the Ross Ice Shelf. At the bottom of the volcano is a small lava lake, which erupted on September 17, 1984, spewing lava out of the main crater. Many small earthquakes have been recorded at seismic stations in this area. Thus far, volcanoes are still an important object for studying strong geological phenomena. It has been found that earthquakes may cause surface subsidence near volcanoes. Takada and Fukushima (2013) and Pritchard (2010) used satellite data to analyze the surface deformation caused by the magnitude 9.0 earthquake in northeastern Japan in 2011 and the magnitude 8.8 earthquake in Maule, Chile in 2010. After these two earthquakes, the highest degree of volcanic subsidence near faults reached 15 cm. The sinking of the volcanoes in Japan was probably caused by the subsidence of magma storage areas under the volcanoes and some brittle hot rocks, while the sinking of the Chilean volcano may have been due to the release of thermal fluids beneath the volcano. Because the stations near Mount Erebus may be affected by underground magmatism, the Ray Seismic Site (RAYG), Nausea Knob (NAUS), Lower Erebus Hut (LEGH), E1 (E1G2), Truncated Cones (CONG) and Hoopers Shoulder (HOOZ) stations, which are within 3 km of Mount Erebus, are extracted and analyzed separately from those stations in the Ross Ice Shelf area. As shown in Figure 3, the GPS stations in this area are all sinking. The RAYG station located in the main crater is experiencing the most serious amount of sinking, with a velocity of −10.80±1.62 mm yr^{-1}. The sinking velocity decreases with increasing distance to the crater. The HOOZ station is approximately 3 km from the crater, and its vertical velocity is −0.32±0.57 mm yr^{-1}. The MCM4* station is ap-

proximately 28 km away from the crater, and its vertical velocity is 0.24±0.26 mm yr^{-1}. The prediction results of the GIA models in this region are all uplift movements. The predicted values of the W12a model are larger than those of the other models and average approximately 4 mm yr^{-1}, and the predicted values of other models are between 0 and 2 mm yr^{-1}. The difference between the GPS-measured vertical velocity (negative value) and the GIA-predicted velocity (positive value) in this area is large, and there is no significant change in the current ice and snow load, which indicates that the subsidence in this area is not caused by the change in the GIA and current ice and snow load but by magmatic activity at the bottom of the volcano.

3.5 Ross Sea coast

Except for the six stations near the volcano, the other GPS stations on the west of the Ross Ice Shelf are all uplifted with a maximum velocity of 3.53 mm yr^{-1} (Mount Coates, COTE), which is in good agreement with most of the predictions of the GIA model, indicating that the uplift movement in this area is mainly affected by GIA. The vertical velocities from the Ramsey Glacier (RAMG), Fallone Nunataks (FALL) and Mount Patterson (PATN) stations are in good agreement with the predicted values from the GIA model. The results indicate that the elevation of these three stations is mainly caused by GIA. For the Clark Mountains (CLRK) and Mount Carbone (MCAR) stations, the vertical velocities and errors estimated by the five-year and seven-year GPS data are 6.11±1.40 and 5.16±2.44 mm yr^{-1}, respectively, which are 2.32 and 3.35 mm yr^{-1} larger than the maximum predictions of the GIA models, respectively. These values also exceed the error ranges of the vertical velocity estimations of the GPS stations. Therefore, the differences should not simply be considered estimation errors in the GPS velocity. Thomas et al. (2011) estimated that the velocities of the two stations were close to 0 mm yr^{-1}, which is quite different from the results of this paper and those from Argus et al. (2014). The reason for these discrepancies may be differences in the time spans of the estimated data. The former uses battle GPS data of less than 200 days from 1998 to 2002, and the latter uses continuous GPS data after 2010. The CLRK and MCAR stations are in the Clarke and Carbone Mountains in the northwestern part of Marie Byrd Land, respectively. The geological structure of the area is stable, and no obvious changes in the current ice and snow load have been found. Therefore, it is possible that GIA models systematically underestimate the GIA uplift in the area. The two IJ05_R2 models are generally lower than the vertical velocity of GPS stations and other GIA models for west of the Ross Ice Shelf, indicating that they may have greater uncertainty in this region.

3.6 West Antarctic inland

The Pecora Escarpment (PECE), Whitmore Mountain (WHTM), Mount Sidley (SDLY) and Mount Howe (HOWE) stations are in the inland of southwest Antarctica. The uplift velocity of GPS is less than 5 mm yr^{-1}, which is in good agreement with most GIA models. At the location of the BENN station, the GIA models differ greatly and the maximum difference reaches 7 mm yr^{-1}, which indicates that there are great uncertainties in the prediction of these GIA models. This station is located in the Bennett Nunataks and was set up in December 2010. The data span is relatively short; thus, these data have not been used to constrain and test the GIA models in previous studies on GIA modeling. In this paper, the vertical velocity of BENN is estimated to be 11.09±1.75 mm yr^{-1} using GPS data from 2010 to 2014, which is faster than the estimates from all the GIA models. The minimum discrepancy in the predicted values of the GIA model is 3.35 mm yr^{-1} (ICE6G_C (VM5a)), and the maximum discrepancy is 10.07 mm yr^{-1} (IJ05_R2 (65 km)). Figure 6 shows the coordinate time series of the station. The time series presents a steady upward trend, no obvious step occurs during the observation period, and the results of curve fitting on the linear and periodic terms are good. Therefore, the GPS velocities of the stations are reliable. No obvious ice mass loss has been found near the station, so it is possible to ignore the influence of current ice and snow load changes. The reason why the GPS lifting velocity is significantly higher than the predicted value of the GIA model may be that the GIA models underestimate the GIA lifting magnitude at this location.

3.7 East Antarctic coast

The vertical velocities at the GPS stations in the coastal area of East Antarctica are between −1.5 and 1.35 mm yr^{-1}, and the average is smaller than that of West Antarctica. The magnitude of the predictions of each GIA model in this region is also relatively small at approximately −1–3 mm yr^{-1}. The basement of East Antarctica is an ancient craton, and the geological structure is very stable; therefore, hardly any vertical movement is caused by geological structural factors in this area. The GRACE gravity data indicate that the ice-snow accumulation rate in the east of Dronning Maud Land and Enderby Land is approximately 150 Gt yr^{-1} from January 2009 to February 2013 (Boening et al., 2012; Argus et al., 2014), totaling approximately 600 Gt. The sedimentary data also indicate that ice and snow accumulated rapidly in this region between 2009 and 2012, although the total accumulation in 1980–2008 was approximately 0 Gt, indicating that the recent accumulation of ice and snow is very abnormal compared to that before 2008. The accumulation of snow and ice caused the coast to sink from 2009 to 2012. The

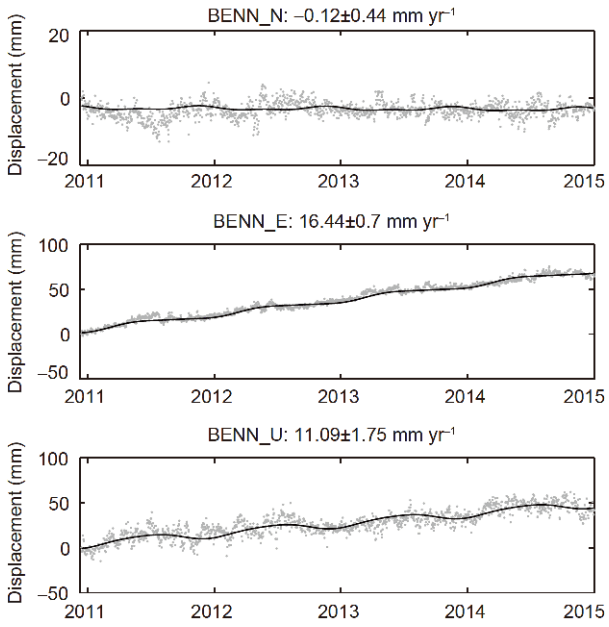

Figure 6 The time series of the station BENN.

GIA model predicts a general uplifting movement. The vertical velocity of the Mawson (MAW1) station on the eastern coast of Enderby Land is −0.72±0.23 mm yr^{-1}, which reflects the vertical velocity of the area. The slight subsidence is caused by the accumulation of ice and snow, although greater uncertainty in each GIA model cannot be ruled out. The ZHON and Davis (DAV1) stations in the Larsemann Hills and the Dumont d'Urville (DUM1) station in Adélie Land are also slightly sinking and have slightly lower velocities than the predictions from the GIA models. The specific reasons remain to be further investigated. The GPS velocities at the Vesleskarvet (VESL) and Syowa (SYOG) stations in the northern part of Dronning Maud Land and that at the Casey (CAS1) station in Vincennes Bay are positive, and the velocities at VESL and SYOG are in good agreement with the predictions from the GIA models. The velocity at the CAS1 station is in good agreement with the ICE-6G (VM5a) and W12a models and has poor consistency with other models. In general, the vertical movement at the stations on the East Antarctic coast is not significant, and it is affected by GIA and changes in the current ice and snow load.

4. Verification and analysis of the GIA model predictions

To visualize the difference between the vertical velocity at GPS stations and those estimated by GIA models, a comparison of the vertical velocity at 58 GPS stations in Antarctica and the predictions from 9 GIA models is shown in Figure 7. The circles of various colors represent the GPS velocity, the background color represents the predictions of GIA models, and the different colors represent the different velocity magnitudes. The closer the colors, the better the consistency between our GPS velocities and the predictions from the GIA models. Figure 7 shows that the color of the stations in the Antarctic Peninsula, the Pine Island Bay along the Amundsen Sea and the Mount Erebus differs greatly from the background color of each GIA model, while in other regions (especially in the East Antarctic coastal region), the color of the stations differs slightly from the background color. The reason for such discrepancies is that the crust of the Antarctic Peninsula, Pine Elan Bay along the Amundsen Sea and the volcanic region of Mount Erebus is not only affected by GIA but also by the obvious changes in the current ice and snow load or underground magmatic activity. To eliminate or weaken the influence of these two factors, we excluded 9 stations in the northern Antarctic Peninsula, 3 stations in Pine Island Bay (BACK, BERP and TOMO) and 6 stations near Mount Erebus when using the vertical velocities at the GPS stations to check the prediction of each GIA model. The remaining 40 stations are located in areas where the current ice and snow load changes are not significant and the geological structure is relatively stable.

The ICE-5G (VM2_L90), Geruo13 (a/b/c) and Paulson07 models are very similar in predicting the spatial distribution of velocity because they all use the same ice model: ICE-5G. Compared with GIA models using other ice models (such as ICE-6G (VM5a), IJ05_R2 and W12a), there are significant differences in the distributions and magnitudes, which indicates that the ice model plays a leading role in the predictions from GIA models. The slight differences among the ICE-5G (VM2_L90), Geruo13 (a/b/c) and Paulson07 models mainly come from different earth models. The ICE-5G (VM2_L90) model uses the VM2 viscous profile and the earth model with a 90-km lithospheric thickness, the Paulson07 model uses a four-layer viscous model that approximates VM2, and the Geruo13 (a/b/c) model uses the VM2 viscous profile and a three-dimensional compressible earth model. It is worth mentioning that these earth models are all one-dimensional models with only the radial variation in the viscosity, and they do not consider the transverse heterogeneity in viscosity. To explore the influence of transverse heterogeneity in the viscosity on GIA prediction, Wang and Wu (2006) and Wang (2009) establishes the GIA model ICE-4G+RF3L20 (β=0.4) with combined constraints on geodetic observations and sea-level data and found that the viscosity of the mantle has significant transverse heterogeneity and a significant influence on GIA predictions. The transverse inhomogeneous viscosity can be obtained by a seismic tomography model. The seismic results from Wilson et al. (2015) also showed that the Antarctic mantle viscosity has

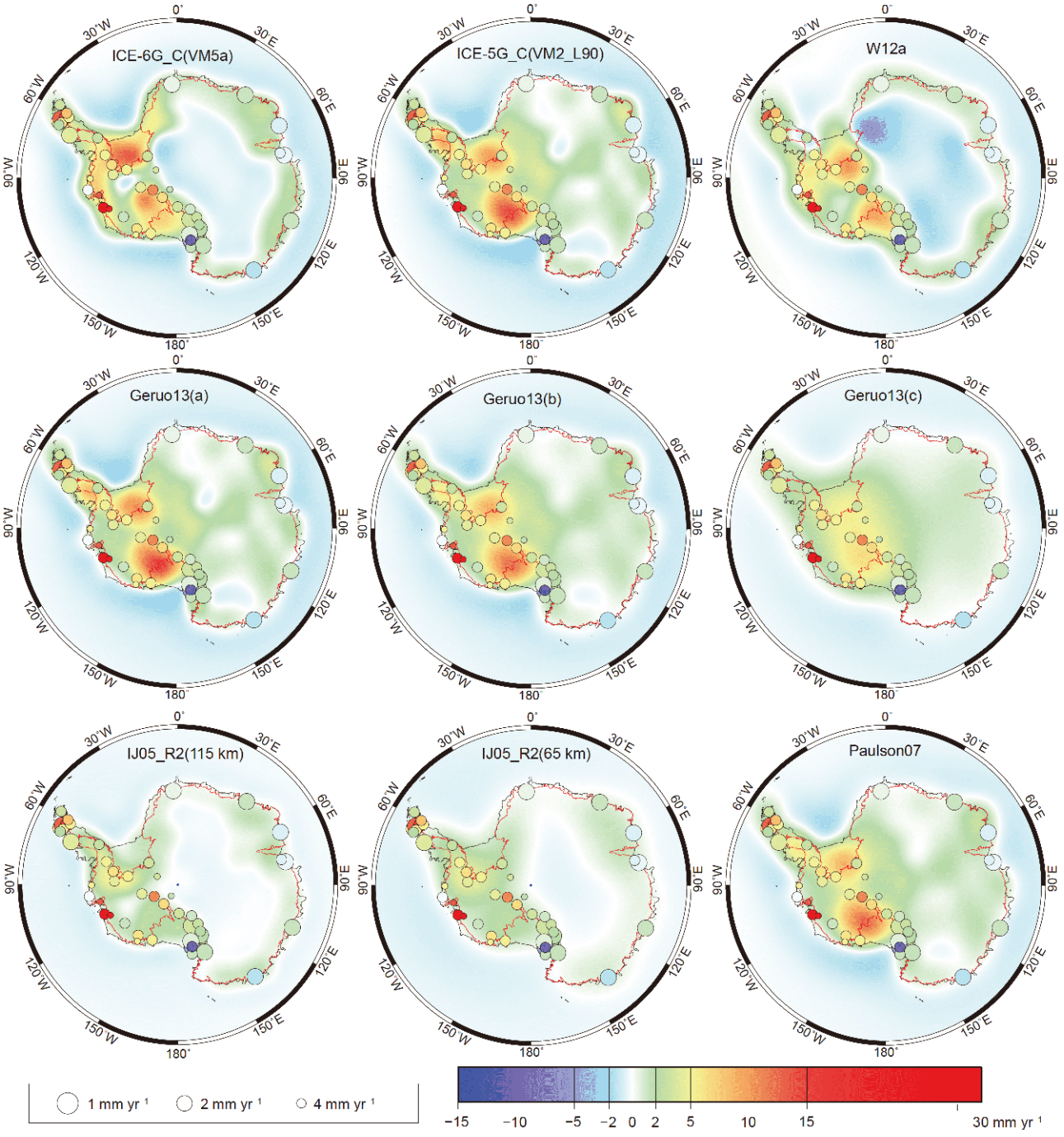

Figure 7 Our GPS vertical velocities (circles) are compared with the predictions of GIA models (background). The color of the circle or the background represents the magnitude, and the size of the circle represents the accuracy of the velocities.

significant and complex transverse changes, which fundamentally affect the isostatic response to the changes in the Antarctic ice and snow mass. Because most GIA models, including ICE-6G (VM5a), do not consider the transverse heterogeneity of viscosity, it is meaningful to determine the real three-dimensional viscosity structure of the mantle for the development of GIA theory and the improvement of models in future GIA model studies.

4.1 Baseline processing

To evaluate the correlation between the vertical velocities of GPS stations and the predictions of each GIA model, we present a linear fitting of the vertical velocity at the GPS stations and the predicted values from each GIA model. The fitting results are shown in Figure 8. The BENN station that deviates the farthest from the fitting line in all the results.

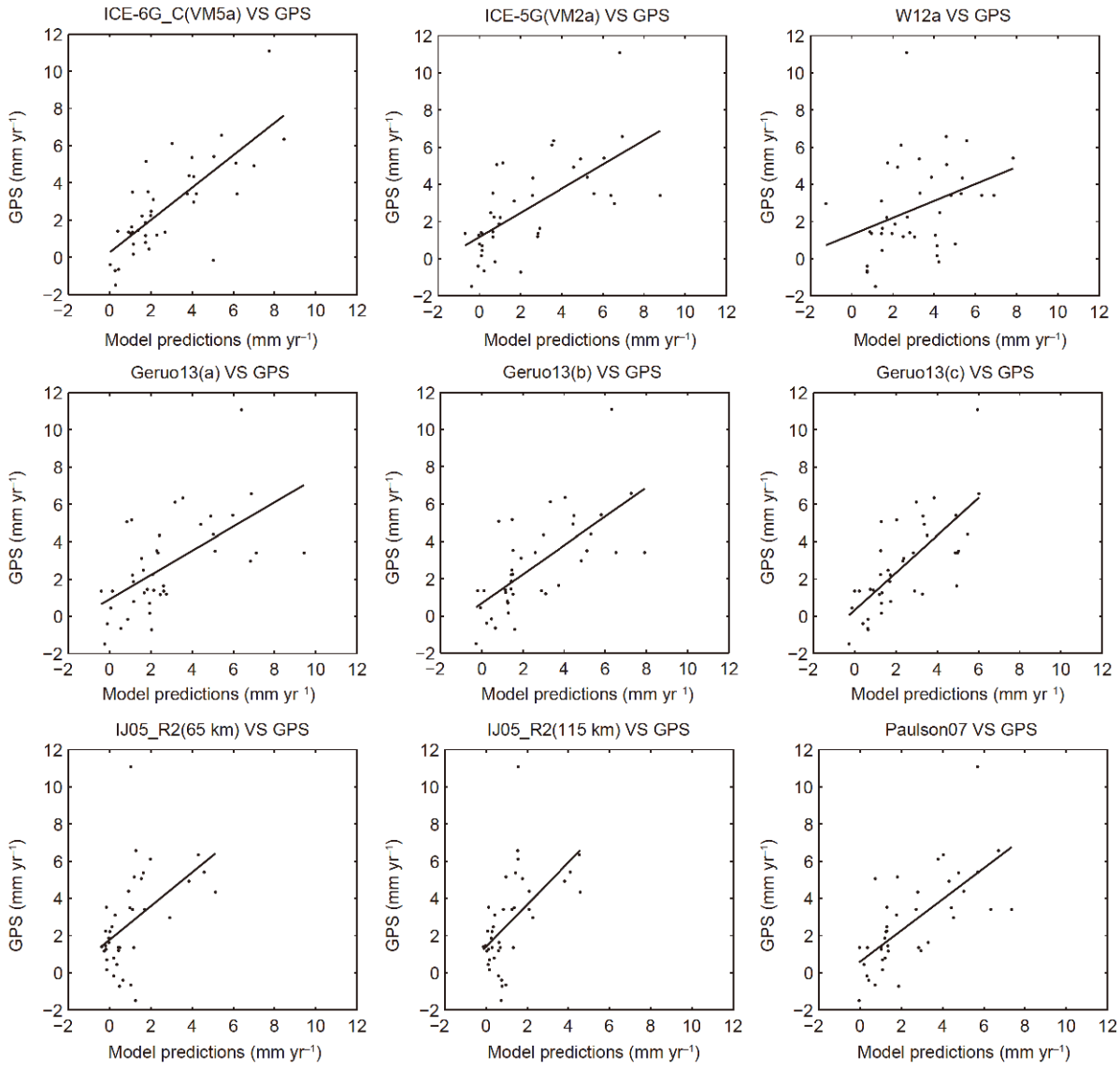

Figure 8 Linear fitting results between our estimated GPS vertical velocities and the GIA model predictions.

The position of the station is also mentioned in section 3.6 of this paper. The vertical velocity at this GPS station is much larger than that predicted by the GIA model, which may be due to the lack of constraints on the measured data in most of the GIA models. Table 2 shows that the vertical velocities at the GPS stations are between 0.45 and 1.13, the intercept is between 0.26 and 1.41, and the correlation coefficient is between 0.35 and 0.76. In theory, if the vertical velocity at a GPS station contains only the response of GIA, the slope and intercept in Figure 8 and Table 2 are 1 and 0, respectively, and the correlation coefficient is 1. Conversely, the closer the slope is to 1, the closer the intercept is to 0, the larger the correlation coefficient, and the higher the coincidence degree between the vertical velocities at the GPS stations and the predictions of the GIA model. The intercept (0.26 mm yr^{-1}) fitted by the vertical velocities at the GPS stations and ICE-

Table 2 Linear fitting parameters and correlation coefficients between our estimated vertical velocities and the GIA model predictions

Model name	Slope	Intercept	Correlation coefficient
ICE-6G_C (VM5a)	0.87	0.26	0.76
ICE-5G (VM2_L90)	0.65	1.17	0.66
W12a	0.45	1.29	0.35
Geruo13 (a)	0.65	0.92	0.60
Geruo13 (b)	0.77	0.69	0.68
Geruo13 (c)	1.01	0.33	0.72
IJ05_R2 (65 km)	0.91	1.77	0.50
IJ05_R2 (11 km)	1.13	1.41	0.56
Paulson07	0.84	0.60	0.69

6G_C (VM5a) is the smallest, and the correlation coefficient (0.76) is the largest. The slope of the fitting between our GPS velocities and Geruo13 (c) is closest to 1 (1.01), and the correlation coefficient is 0.72. This finding means that our GPS velocities present the best agreement with the predictions from the two GIA models. The linear fitting and the correlation coefficients between the vertical velocities of the GPS stations and the predictions of the GIA model can reflect the uncertainty in the GIA model to some extent. Next, we focus on the analysis of the uncertainty in each GIA model.

4.2 Uncertainty analysis of the GIA models

The uncertainty in the GIA model mainly comes from two aspects: the inaccuracy of the ice sheet thickness history in the ice model and the considerable simplification of the earth model. Both Laurentia and the Fennoscandia are now inland seas, i.e., Hudson Bay and Bosnia Bay, respectively. After the glacial period, many Holocene coastlines appeared, which strongly constrained the glacial history and mantle viscosity. In contrast, the lack of accurate historical relative sea-level (RSL) data on the maximum thickness area of the ice sheet in Antarctica will lead to nonunique ice models and a lack of geodetic data for the constrained model in Antarctica and the elastic response caused by the current ice and snow load changes; moreover, the reconstruction of the ice loss history in Antarctica is more complex than that of Laurentia or Fennoscandia. For a long time, the errors in GIA models were either not given or quantified by differences between models. For example, the W12a model uses a series of different ice models to quantify the errors, whereas Geruo13 and IJ05_R2 also use a series of different earth models when quantifying the errors but neither method is able to accurately reflect the real uncertainty, especially when the GRACE data are corrected by GIA models, which will lead to systematic errors rather than random errors.

To analyze the real uncertainties in different GIA models, we take the vertical velocity at the GPS stations as a reference, determine the discrepancies between the vertical velocities at the GPS stations and the GIA model predictions, and count the number of discrepancies in different intervals. Considering the great difference between East and West Antarctica, the distributions of discrepancies between our GPS vertical velocities in East and West Antarctica and the GIA model predictions are given in Figure 9. The length of each interval is 1 mm yr^{-1}. East Antarctica includes 7 stations along the East Antarctic coast and 15 stations west of the Ross Ice Shelf, totaling 22 stations. The West Antarctic stations include 6 stations on the Filchner-Ronne Ice Shelf, 2 stations along the Amundsen Sea (excluding Pine Island Bay), 5 stations on the east coast of the Ross Ice Shelf and 5 stations in inland West Antarctica, totaling 18 stations. Figure 9 shows that the distribution of discrepancies in East Antarctica is concentrated and the range of discrepancies is between −4 and 4 mm yr^{-1}, while the distribution of discrepancies in West Antarctica is scattered and the range of discrepancies is between −6 and 10 mm yr^{-1}. These findings mean that the uncertainty in each GIA model in West Antarctica is generally greater than that in East Antarctica.

Table 3 gives the comparison of the weighted mean value and WRMS of the differences between our GPS vertical velocities and the predictions from GIA models. The weighted mean of the difference can test whether there is systematic deviation between the two, and the WRMS of the difference can effectively measure the magnitude of the deviation between the two. Table 3 shows that the weighted mean of discrepancies is greater than or equal to 0 in West Antarctica, indicating that the GPS results in West Antarctica are larger than those predicted by the GIA models, whereas both positive and negative values in East Antarctica, with the negative values indicating that the predicted values from the ICE-6G_C (VM5a), W12a and Geruo13 (a) models in East Antarctica are larger than those predicted by GPS. The total weighted mean values of the vertical velocity from GPS are 1.55 and 1.67 mm yr^{-1} in West Antarctica and East Antarctica, respectively, which indicate that the predictions of the two GIA models are systematically smaller than the GPS vertical velocities. The total weighted mean of the difference between the vertical velocity from GPS and the W12a model is −0.39 mm yr^{-1}, which indicates that the predictions of the W12a model are systematically larger than the GPS vertical velocities. The weighted mean magnitude of the difference between the GPS vertical velocities and those predicted by the ICE-6G_C (VM5a), ICE-5G (VM2_L90), Geruo13 series and Paulson07 models is relatively small, which indicates that the predictions from the GIA models are generally unbiased from the GPS vertical velocities. The WRMS of the vertical velocities in West Antarctica is generally larger than that of East Antarctica, which is consistent with the conclusion in Figure 9. The WRMS (0.88 mm yr^{-1}) of the difference between the vertical velocities and the predictions of ICE-6G_C (VM5a) is the smallest, followed by the WRMS (1.15 mm yr^{-1}) of the difference between the vertical velocities and the predictions of Geruo13 (c), and the WRMS (2.10 and 2.01 mm yr^{-1}) of the difference between the vertical velocities and the predictions of IJ05_R2 is the largest. Therefore, taking our GPS vertical velocities as a reference, we conclude that the ICE-6G_C (VM5a) model has the lowest uncertainty in the above regions, followed by the Geruo13 (c) model, while the IJ05_R2 model has the greatest uncertainty. The minimum uncertainty in the ICE-6G_C (VM5a) model may be related to the data set used for the constraining model. This model uses the vertical velocities of 42 GPS stations estimated by Argus et al. (2014) as a constraint, while other models, such as W12a and IJ05_R2, used

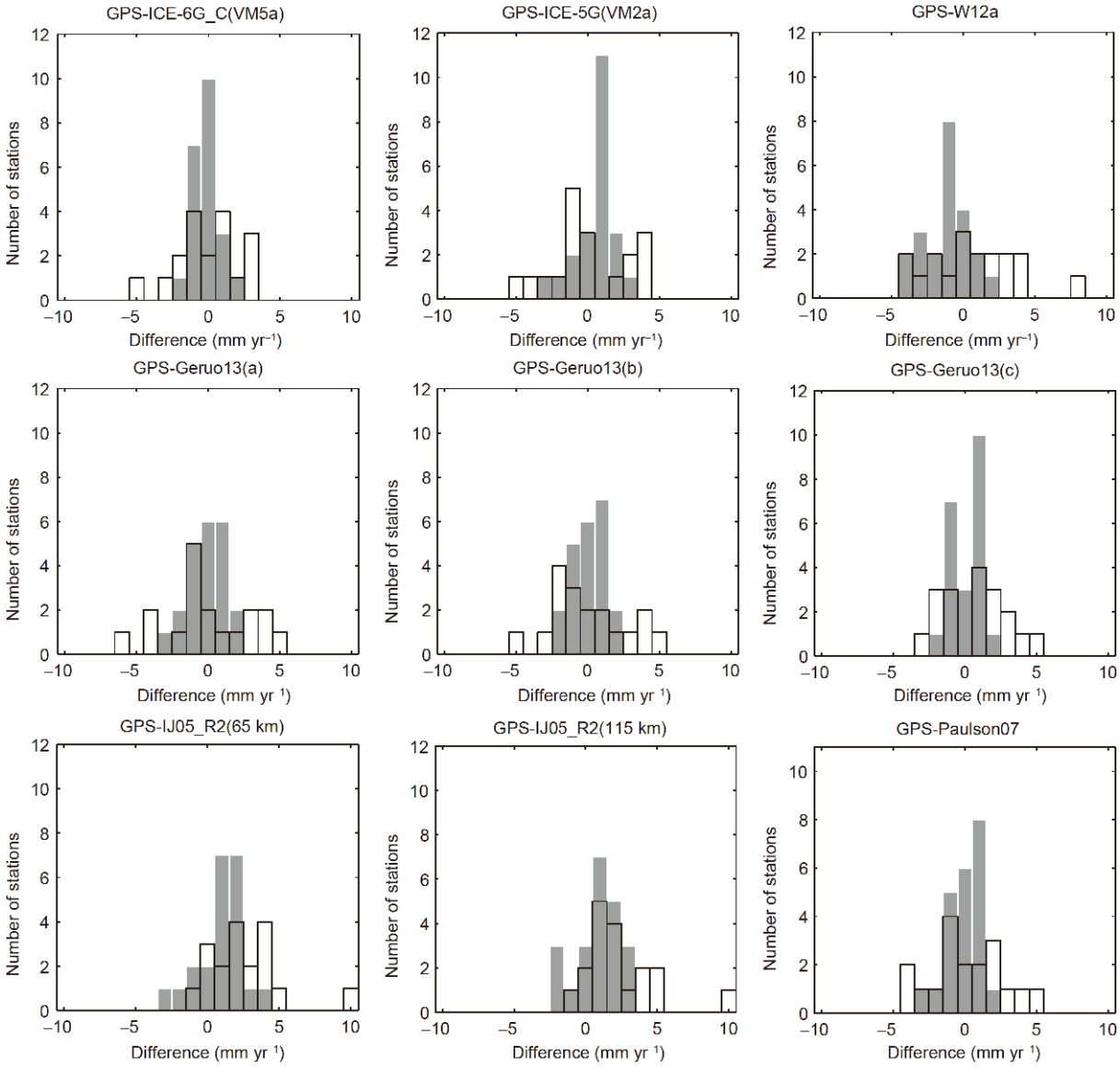

Figure 9 The distribution of differences between our vertical velocities to the predictions of each GIA model in East Antarctica (gray solid) and West Antarctica (black hollow), respectively. The interval length is 1 mm yr^{-1}.

Table 3 The weighted mean residuals and WRMS residuals of our vertical velocities to the predictions of each GIA model

GPS-GIA	Weighted mean residual (mm yr^{-1})			WRMS residual (mm yr^{-1})		
	East	West	Total	East	West	Total
GPS-ICE-6G_C (VM5a)	−0.18	0.00	−0.10	0.75	2.08	0.88
GPS-ICE-5G (VM2_L90)	0.59	0.04	0.34	1.48	2.59	1.53
GPS-W12a	−1.27	0.68	−0.39	1.26	3.08	1.67
GPS-Geruo13 (a)	−0.15	0.09	−0.04	1.42	2.85	1.53
GPS-Geruo13 (b)	0.04	0.17	0.10	1.26	2.32	1.33
GPS-Geruo13 (c)	0.03	0.69	0.33	1.05	1.89	1.15
GPS-IJ05_R2 (a)	0.98	2.51	1.67	1.67	2.42	2.10
GPS-IJ05_R2 (b)	0.85	2.41	1.55	1.55	2.28	2.01
GPS-Paulson07	0.06	0.35	0.19	1.31	2.22	1.39

the earlier Thomas et al. (2011) GPS data set as a constraint.

The uncertainty in the GIA model may be affected by different parameters in the earth models. The three earth models of the Geruo13 series mainly differ in the truncation order and Gaussian filter radius, which lead to three different prediction results. From the WRMS in Table 3 and the correlation coefficients in Table 2, we can see that as the truncation order decreases and the Gaussian filter radius increases, the WRMS decreases and the correlation coefficient increases; that is, the predicted velocity is closer to the vertical velocity at the GPS station. The vertical velocity at the station may be due to larger errors in the higher-order terms of the model, which can be effectively reduced by truncating to a lower order and performing Gaussian filtering. The two models of the IJ05_R2 series mainly differ in lithospheric thickness and lower mantle viscosity. From the WRMSs in Table 3 and the correlation coefficients in Table 2, the IJ05_R2 (115 km) model with larger lithospheric thickness and lower mantle viscosity is closer to the GPS results.

Although the current Antarctic GIA model has been greatly improved over previous versions (e.g., the uncertainty in ICE-6G_C (VM5a) is significantly reduced compared with ICE-5G (VM2_L90)), the status of Antarctic GIA modeling is still not optimistic. In North America, the WRMS of the difference between the GPS results calculated by Park et al. (2002) and the predictions from the improved earth model ICE-3G is 0.42 mm yr^{-1}. The correlation coefficient between the VLBI results calculated by Zhu et al. (2005) and the ICE-4G model is 0.89, and the difference in the WRMSs is 0.8 mm yr^{-1}. The latest ICE-6G_C (VM5a) model has been greatly improved over the ICE-3G and ICE-4G models (Peltier et al., 2015). In Antarctica, the correlation coefficients between the GPS results and the GIA models ranged from 0.35 to 0.76, and the WRMS of the difference between the GPS results and the GIA models ranged from 0.88 to 2.10 mm yr^{-1}. Therefore, compared with North America, the correlation coefficient between the predictions of the GIA model and the GPS vertical velocities in Antarctica is generally low and the difference in the WRMSs is larger. At certain stations where the variation in the ice and snow load is not significant (such as BENN), the GPS vertical velocities are quite different from those at other stations. However, in areas where the variation in the ice and snow load is significant (such as the northern Antarctic Peninsula and Pine Island Bay along the Amundsen Sea), there is no direct GPS constraint and the uncertainty in the elastic correction models is high.

5. Conclusions

Using GAMIT/GlOBK10.5, data from 73 GPS stations in Antarctica and its surrounding areas from 1996 to 2014 were analyzed, and the baseline solutions (h files) of the global network IGS1-IGS9 were adjusted jointly to obtain the daily coordinate time series for each station. The outliers in the coordinate time series were eliminated using the interquartile criterion. The steps in the time series from certain stations were estimated and corrected by CATS. Considering the WN, FN and RWN, the maximum likelihood estimation method in CATS is used to estimate the velocity and uncertainty at each station, and the velocities of colocated or adjacent stations are merged.

In this paper, our GPS vertical velocities are compared with those estimated by Argus et al. (2014) and Thomas et al. (2011) and the predictions from nine GIA models. Significant elastic uplift was caused by the changes in the ice and snow load in the north Antarctic Peninsula and Pine Island Bay along the Amundsen Sea, and significant crustal subsidence at Mount Erebus may be related to volcanic underground magmatism. The vertical velocities at GPS stations along the coast of East Antarctica are not significant. The vertical movements at stations in other areas are mainly affected by GIA.

An analysis of the correlation between the GPS results and GIA models, as well as the uncertainty in the GIA models, showed that the ICE-6G (VM5a) model is the most consistent with our vertical velocities, followed by the Geruo13 model. The W12a and IJ05_R2 series models have relatively poor consistency with our GPS results. At present, these new GIA models for Antarctica have been greatly improved over previous models, however, the conditions of GIA modeling in Antarctica are still not optimistic compared with other regions such as North America. With the continuous expansion of the geodetic data set in Antarctica, and the improvements in GIA theoretical and modeling methods, such as the transverse inhomogeneity in the mantle viscosity, this situation will be improved.

Acknowledgements *We thank MIT/SIO for provision of GAMIT/GLOBK software suit; IGS, POLENET for IGS and POLENET GPS data (all these data are downloaded from the FTP service garner.ucsd.edu/pub/), CACSM (Chinese Antarctica Center of Surveying and Mapping) for data of ZHON; and all the researchers and agents for the GIA models used in this study. This work was supported by the National Key Research and Development Program of China (Grant No. 2017YFA0603104), the State Key Program of the National Natural Science Foundation of China (Grant No. 41531069), and the Independent Scientific Research Program for Cross-disciplinary of Wuhan University (Grant No. 2042017kf0209).*

References

Altamimi Z, Collilieux X. 2009. IGS contribution to the ITRF. J Geod, 83: 375–383

Argus D F, Peltier W R, Drummond R, Moore A W. 2014. The Antarctica component of postglacial rebound model ICE-6G_C (VM5a) based on GPS positioning, exposure age dating of ice thicknesses, and relative sea level histories. Geophys J Int, 198: 537–563

Argus D F, Peltier W R. 2010. Constraining models of postglacial rebound using space geodesy: A detailed assessment of model ICE-5G (VM2) and its relatives. Geophys J Int, 107: 697–723
Blewitt G, Lavallée D. 2003. Effect of annual signals on geodetic velocity. J Geophys Res, 108: 2010
Boening C, Lebsock M, Landerer F, Stephens G. 2012. Snowfall-driven mass change on the East Antarctic ice sheet. Geophys Res Lett, 39: L21501
E Dong Chen, Zhang S K. 2006. Infrastructure and progress of international Antarctic geodetic reference framework (in Chinese). J Geodesy Geody, 26: 104–108
Geruo A, Wahr J, Zhong S. 2013. Computations of the viscoelastic response of a 3-D compressible Earth to surface loading: An application to Glacial Isostatic Adjustment in Antarctica and Canada. Geophys J Int, 192: 557–572
Ivins E R, James T S, Wahr J, Schrama O E J, Landerer F W, Simon K M. 2013. Antarctic contribution to sea level rise observed by GRACE with improved GIA correction. J Geophys Res-Solid Earth, 118: 3126–3141
Jiang W P, Zhou X H. 2015. Effect of the span of Australian GPS coordinate time series in establishing an optimal noise model. Sci China Earth Sci, 58: 523–539
Jiang W, Zhao Q, Liu H, Yang K. 2011. Application of the sub-network division in large scale GNSS reference station network (in Chinese). Geomat Inform Sci Wuhan Univ, 36: 389–391
King M A, Altamimi Z, Boehm J, Bos M, Dach R, Elosegui P, Fund F, Hernández-Pajares M, Lavallee D, Mendes Cerveira P J, Penna N, Riva R E M, Steigenberger P, van Dam T, Vittuari L, Williams S, Willis P. 2010. Improved constraints on models of glacial isostatic adjustment: A review of the contribution of ground-based geodetic observations. Surv Geophys, 31: 465–507
King M A, Santamaría-Gómez A. 2016. Ongoing deformation of Antarctica following recent great earthquakes. Geophys Res Lett, 43: 1918–1927
Li W, Ju X, Shen Y, Zhang Z. 2014. Vertical deformation analysis of Antarctic GNSS stations combined using GNSS and GRACE data. Chin J Polar Res, 26: 238–243
Li F, Ma C, Zhang S K, Lei J, Hao W, Zhang Q, Li W. 2016. Noise analysis of the coordinate time series of the continuous GPS station and the deformation patterns in the Antarctic Peninsula (in Chinese). Chin J Geophys, 59: 2402–2412
Ma C, Li F, Zhang S K, Lei J, E D, Hao W, Zhang Q. 2016. The coordinate time series analysis of continuous GPS stations in the Antarctic Peninsula with consideration of common mode error (in Chinese). Chin J Geophys, 59: 2783–2795
Milne G A, Davis J L, Mitrovica J X, Scherneck H G, Johansson J M, Vermeer M, Koivula H. 2001. Space-geodetic constraints on glacial isostatic adjustment in Fennoscandia. Science, 291: 2381–2385
Mitrovica J X, Gomez N, Clark P U. 2009. The sea-level fingerprint of West Antarctic collapse. Science, 323: 753
Nield G, Whitehouse P, King M, Clarke P. 2015. Glacial Isostatic Adjustment on the Siple Coast. Vienna: EGU General Assembly Conference Abstracts, 17: 10494
Nikolaidis R. 2002. Observation of geodetic and seismic deformation with the Global Positioning System. Dissertation for Doctoral Degree. San Diego: University of California
Park K D, Nerem R S, Davis J L, Schenewerk M S, Milne G A, Mitrovica J X. 2002. Investigation of glacial isostatic adjustment in the northeast U. S. using GPS measurements. Geophys Res Lett, 29: 1509
Paulson A, Zhong S, Wahr J. 2007. Inference of mantle viscosity from GRACE and relative sea level data. Geophys J Int, 171: 497–508
Peltier W R. 2004. Global glacial isostasy and the surface of the ice-age Earth: The ICE-5G (VM2) model and GRACE. Annu Rev Earth Planet Sci, 32: 111–149
Peltier W R, Argus D F, Drummond R. 2015. Space geodesy constrains ice age terminal deglaciation: The global ICE-6G_C (VM5a) model. J Geophys Res-Solid Earth, 120: 450–487
Prandi P, Cazenave A, Becker M. 2009. Is coastal mean sea level rising faster than the global mean? A comparison between tide gauges and satellite altimetry over 1993–2007. Geophys Res Lett, 36: L05602
Pritchard M. 2010. Deformation explained. Nat Geosci, 3: 515
Takada Y, Fukushima Y. 2013. Volcanic subsidence triggered by the 2011 Tohoku earthquake in Japan. Nat Geosci, 6: 637–641
Thomas I D, King M A, Bentley M J, Whitehouse P L, Penna N T, Williams S D P, Riva R E M, Lavallee D A, Clarke P J, King E C, Hindmarsh R C A, Koivula H. 2011. Widespread low rates of Antarctic glacial isostatic adjustment revealed by GPS observations. Geophys Res Lett, 38: L22302
Wang H. 2009. Glacial isostatic adjustment model constrained by geodetic measurements and relative sea level. Chin J Geophys, 52: 2450–2460
Wang H, Wu P. 2006. Effects of lateral variations in lithospheric thickness and mantle viscosity on glacially induced surface motion on a spherical, self-gravitating Maxwell Earth. Earth Planet Sci Lett, 244: 576–589
Wang H, Wu P, van der Wal W. 2008. Using postglacial sea level, crustal velocities and gravity-rate-of-change to constrain the influence of thermal effects on mantle lateral heterogeneities. J Geodyn, 46: 104–117
Whitehouse P L, Bentley M J, Le Brocq A M. 2012a. A deglacial model for Antarctica: Geological constraints and glaciological modelling as a basis for a new model of Antarctic glacial isostatic adjustment. Quat Sci Rev, 32: 1–24
Whitehouse P L, Bentley M J, Milne G A, King M A, Thomas I D. 2012b. A new glacial isostatic adjustment model for Antarctica: Calibrated and tested using observations of relative sea-level change and present-day uplift rates. Geophys J Int, 190: 1464–1482
Wilson T J, Bevis M, Konfal S, Barletta V, Aster R, Chaput J, Heeszel D, Wiens D, Anandakrishnan S, Dalziel I, Huerta A, Kendrick E, Nyblade A, Winberry P, Smalley B, Lloyd A. 2015. Understanding glacial isostatic adjustment and ice mass change in Antarctica using integrated GPS and seismology observations. Vienna: EGU General Assembly Conference Abstracts. 17: 7762
Wu P, Wang H. 2006. Effects of mode coupling and location of rotational axis on glacial induced rotational deformation in a laterally heterogeneous viscoelastic earth. Geophys J Int, 167: 853–859
Zhu X H, Sun F P. 2005. Detection of postglacial rebound by using VLBI data (in Chinese). Chin J Geophys, 48: 308–313

(Responsible editor: Xin LI)